Dihydroindeno[2,1-*c*]fluorene-Based Imide Dyes: Synthesis, Structures, Photophysical and Electrochemical Properties

Yang-Yang Li,[†,‡] Hai-Yan Lu,*,[‡] Meng Li,[†,‡] Xiao-Jun Li,*,[†,‡] and Chuan-Feng Chen*,[†]

[†]Beijing National Laboratory for Molecular Sciences, CAS Key Laboratory of Molecular Recognition and Function, Institute of Chemistry, Chinese Academy of Sciences, Beijing 100190, China

[‡]University of Chinese Academy of Sciences, Beijing 100049, China

Ⓢ *Supporting Information*

ABSTRACT: A new kind of imide dyes based on dihydroindeno[2,1-*c*]fluorene have been developed. Consequently, a series of the organic dyes were conveniently and efficiently synthesized. The single crystal structure showed the dihydroindeno[2,1-*c*]fluorene core was almost planar, and the dye molecule could pack into herringbone-like structure in the solid state. It was found that the imide dyes all showed strong fluorescence emissions in tetrahydrofuran, and they also exhibited obvious red shifts with the increase of the π-conjugation system and the enhancement of the electronic-donating effect. Moreover, the electrochemical cyclic voltammograms of the imide dyes displayed irreversible redoxes in the film state. The electronic structures of aryl substituted imide dyes were also studied by the density functional theory (DFT), which gave a further explanation for their electrochemical behaviors.
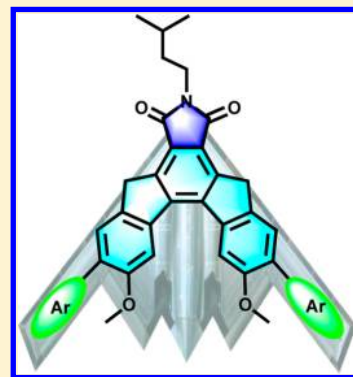
INTRODUCTION

Dihydroindenofluorenes are a class of scaffold-shaped polycyclic aromatic hydrocarbons (PAHs) that consist of terphenyl bridged by two methylene groups.[1] Its chemistry has not been well developed[2] since Gabriel synthesized the first indenofluorene dione in the late nineteenth century.[3] Until very recently the dihydroindenofluorenes were identified as a semiconducting material in devices,[3−5] and since then the molecules with dihydroindenofluorene frameworks have been attracting more and more attention.[6−9] The dihydroindenofluorene family is comprised of five constitutional isomers,[1] among which most of the researches were focused on the dihydroindeno[1,2-*b*]fluorene for its simple and high-yield synthetic routes.[10−12] However, the studies on the other kinds of dihydroindenofluorenes were rather limited. Therefore, it is of great importance to have a more comprehensive understanding on other kinds of dihydroindenofluorene systems.

Among all the dihydroindenofluorene isomers, dihydroindeno[2,1-*c*]fluorene is the only one that possessed helicene-like structure with *ortho*-fused aromatic rings.[1−3,13] Although Haley group recently reported the first example of a fully conjugated indeno[2,1-*c*]fluorene, and the X-ray crystal structures of the *P*- and *M*-enantiomers were also shown,[2,3] almost no dihydroindeno[2,1-*c*]fluorene derivatives with a unique structure have been reported so far[14−18] probably due to their synthetic difficulties, such as complicated precursors, harsh reaction conditions, and difficulties for further functionalization.

Imides, as a kind of common electronic-withdrawing group, are often fused with electronic-rich π-conjugated structures, such as perylene, naphthalene, and anthracene, to form different organic dyes like perylene-3,4-dicarboximides (PMIs),[19,20] perylene-3,4:9,10-bis(dicarboximides) (PDIs),[21−23] naphthalene-1,8-dicarboximides (NMI),[24] naphthalene-1,4:5,8-bis-(dicarboximides) (NDI),[25−27] and anthracene diimide.[28,29] These imide dyes have been applied in wide research areas including fluorescent sensing and imaging,[30] and dye-sensitized solar cells[31−33] for their good stability, high electron affinities, and charge transmission ability.[34,35] We deduced that by the combination of imide moiety and dihydroindeno[2,1-*c*]fluorene core, a new kind of organic dyes could be developed. In this paper, we report (1) the convenient and efficient synthesis of a series of imide dyes based on dihydroindeno[2,1-*c*]fluorene core; (2) the crystal structure of the dye containing two 3-thienyl groups and its assembly in the solid state; (3) the strong fluorescence emissions of the imide dyes in tetrahydrofuran; (4) the electrochemical properties of the imide dyes in the film state; and (5) their electronic structures studied by the density functional theory (DFT).
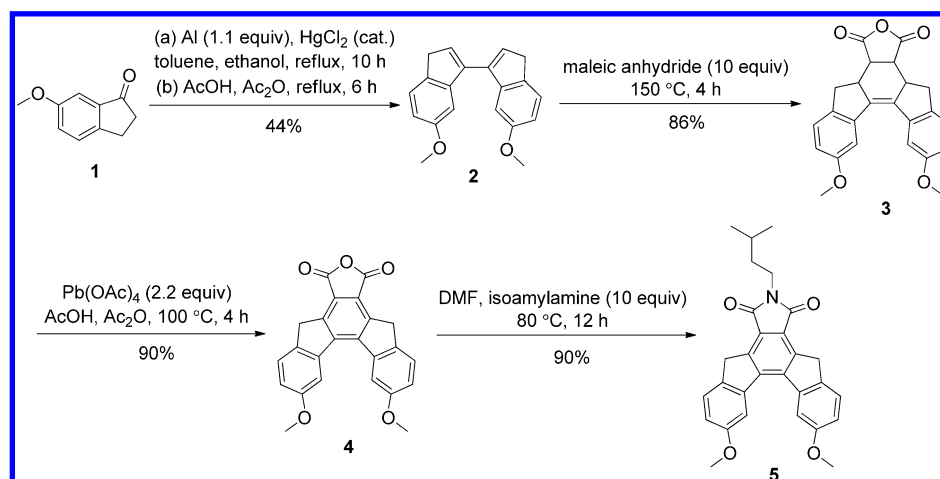
RESULTS AND DISCUSSION

Synthesis of the Imide Dyes. Synthesis of imide **5** is depicted in Scheme 1. Starting from the commercially available 6-methoxy-2,3-dihydro-1*H*-inden-1-one **1**, diene **2** was obtained in 44% yields for two steps. The Diels−Alder reaction between diene **2** and maleic anhydride gave product **3** in 86% yield, which then underwent the dehydrogenation with lead tetraacetate as the oxidant to give the anhydride **4** in 90% yield.

Scheme 1. Synthesis of Imide 5

Scheme 2. Synthesis of Imide Dyes 8a−n

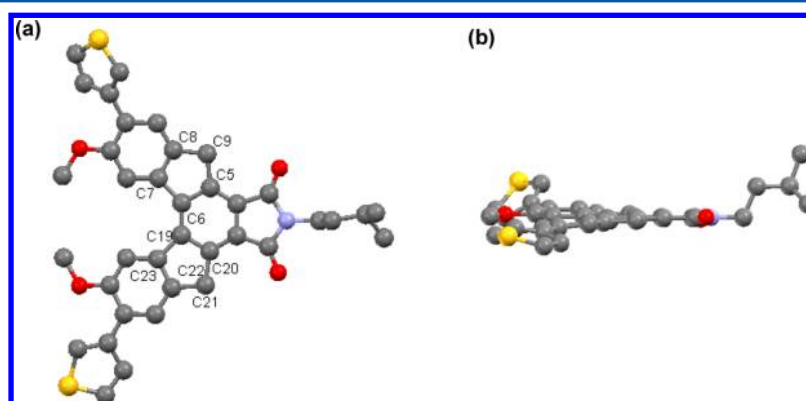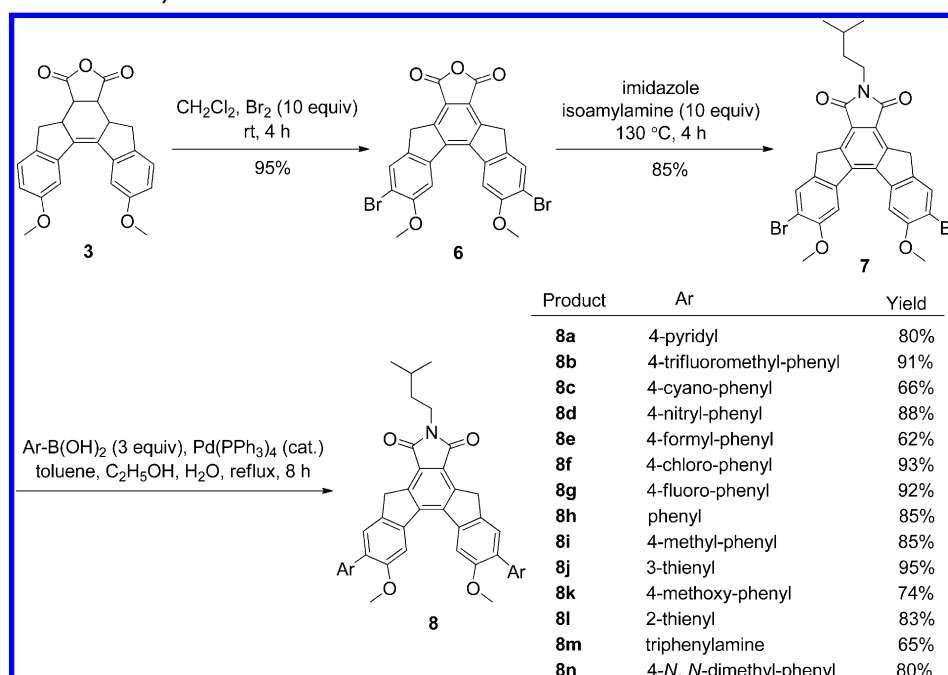| Product	Ar	Yield
8a	4-pyridyl	80%
8b	4-trifluoromethyl-phenyl	91%
8c	4-cyano-phenyl	66%
8d	4-nitryl-phenyl	88%
8e	4-formyl-phenyl	62%
8f	4-chloro-phenyl	93%
8g	4-fluoro-phenyl	92%
8h	phenyl	85%
8i	4-methyl-phenyl	85%
8j	3-thienyl	95%
8k	4-methoxy-phenyl	74%
8l	2-thienyl	83%
8m	triphenylamine	65%
8n	4-*N*, *N*-dimethyl-phenyl	80%

Figure 1. (a) Top view and (b) side view of crystal structure of **8j**. Hydrogen atoms are omitted for clarity.

Finally, imide **5** was obtained in 90% yield by the reaction of **4** with isoamylamine in DMF under argon.

As shown in Scheme 2, when acid anhydride **3** underwent the dehydrogenation by bromine in dichloromethane, it was

found that the dibromo-substituted anhydride **6** could be obtained in 95% yield. Compound **6** is an excellent precursor for the further functionalization. Consequently, the reaction of **6** with isoamylamine in the presence of imidazole gave the
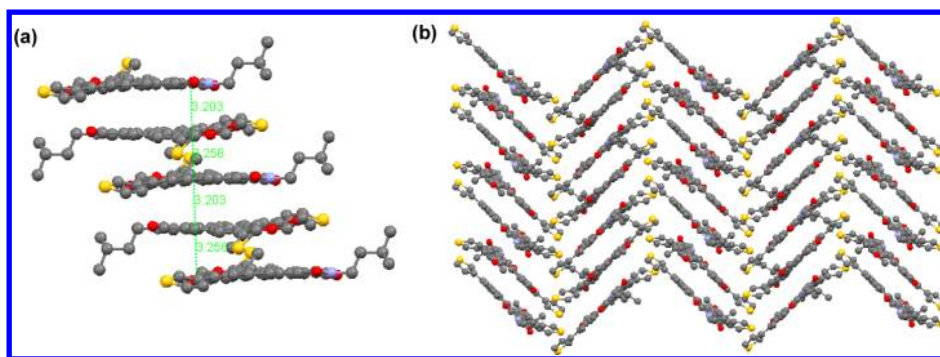
Figure 2. (a) Head to tail arrangement of molecule **8j**, and (b) its herringbone-like packing viewed along the *a* axis.

dibromo-substituted imide **7** in 85% yield, which then underwent Suzuki–Miyaura cross-coupling reactions with a variety of boric acids to give diaryl-substituted imide dyes **8a–n** in 62–95% yields. All of these new imide dyes showed good solubility in common organic solvents including toluene, DCM, THF, EA, TCM, and DMSO at room temperature.

Crystal Structure of Imide Dye 8j. A single crystal of **8j** suitable for X-ray diffraction was obtained by slow evaporation of its solution in chloroform and cyclohexane. The crystal structure was shown in Figure 1. It was found that the torsion angle of C7–C6–C19–C23 was 4.90°, indicating that the dihydroindeno[2,1-*c*]fluorene core had an approximate plane structure. The bond lengths of C8–C9 (1.50 Å), C5–C9 (1.49 Å); C20–C21 (1.50 Å), C21–C22 (1.49 Å) were all shorter than the C–C single bond (1.54 Å), but longer than the C–C double bond (1.34 Å), suggesting that the electrons in the dihydroindeno[2,1-*c*]fluorene core were delocalized. Moreover, it was also found that by the head to tail arrangement (Figure 2a) with the distances of 3.20 and 3.26 Å between the adjacent molecules, molecule **8j** could pack into a herringbone-like structure (Figure 2b).

Photophysical Properties. In order to explore the influence of solvents on the imide dyes, we first investigated the photophysical properties of the phenyl substituted derivative **8h** in different solvents, and the results were summarized in Table 1. It was found that the maximum

Table 1. Photophysical Data of 8h in Different Solvents

solvent[a]	λ_{abs} (nm)[b]	log ε	λ_{em} (nm)[c]	$\Delta\lambda_{stokes}$ (nm)[d]	Φ_f[e]	τ_f (ns)[f]
toluene	376, 405	4.40, 4.38	460	55	0.48	2.55
DCM	376, 411	4.38, 4.36	489	78	0.63	5.64
THF	375, 408	4.42, 4.41	469	61	0.55	3.71
EA	374, 405	4.41, 4.40	468	63	0.61	3.99
TCM	377, 414	4.35, 4.34	492	78	0.64	5.95
acetone	375, 407	4.43, 4.43	486	79	0.38	5.36
ACN	375, 406	4.41, 4.38	497	91	0.46	6.33
DMSO	377, 413	4.35, 4.36	503	90	0.47	6.41

[a]DCM: dichloromethane; THF: tetrahydrofuran; EA: ethyl acetate; TCM: trichloromethane; ACN: acetonitrile; DMSO: dimethyl sulfoxide. [b]The maximum absorption bands more than 300 nm. [c]Excited at the longest maximum absorption band. [d]Stokes shift = $\lambda_{max}^{em} - \lambda_{max}^{abs}$. [e]Perylene as the standard (cyclohexane, 0.98).[36,37] [f]Fluorescent lifetime.

absorption of **8h** at the concentration of 1×10^{-5} M changed slightly from toluene to DMSO. On the contrary, its fluorescence emission spectra showed obvious solvatochromism. As shown in Figure 3a, the fluorescence spectra of **8h** in
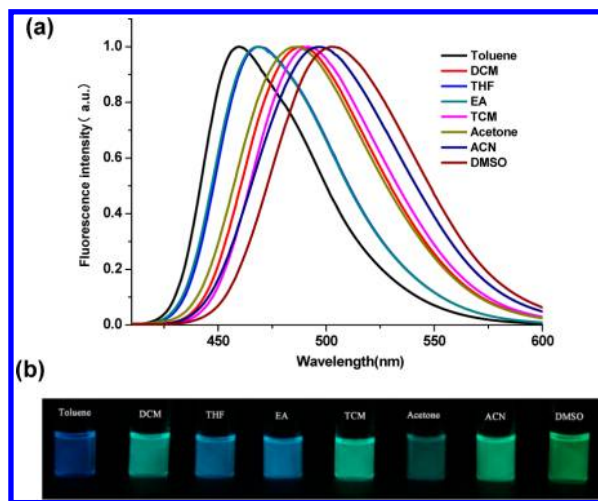

Figure 3. (a) Fluorescence spectra of **8h** in different solvents (1×10^{-5} M), and (b) images for the fluorescent colors of **8h** in corresponding solution under ultraviolet light (365 nm).

different solvents (1×10^{-5} M) showed that by increasing the polarity of the solvent, the maximum emission band increased from 460 nm (toluene) to 503 nm (DMSO). And the Stokes shift also changed largely from less polar solvent (toluene 55 nm) to more polar solvent (ACN 91 nm and DMSO 90 nm). Moreover, the fluorescence lifetime (τ_f) showed that with the increase of the solution polarity, the life expectancy also increases dramatically from 2.55 ns (toluene) to 6.41 ns (DMSO). These results indicated that **8h** showed not only a polar character but also a strong push–pull electronic effect in the excited state compared with those ones in its ground state. Furthermore, it was found that the fluorescence color of **8h** under ultraviolet light (365 nm) could be changed from blue in toluene to green in DMSO, and these color changes in different solvents could be visually seen as well (Figure 3b).

The photophysical properties of the imide dyes **8a–n** with different aromatic groups in THF at a concentration of 1×10^{-5} M were further investigated in details, and the photophysical data were summarized in Table 2. In the UV–vis absorption spectra (Figures S40–S42, Supporting Information), two absorption bands were observed in general. A narrow one located at 250–320 nm, which may be caused by the π–π* transition absorption of conjugated diene in the benzene ring, and a wide one located at 320–440 nm, which may be caused by the π–π* transition absorption of the big conjugate system, and that was common in the push–pull type molecules.[9,38] Moreover, it was also found that with the increase of the

Table 2. Photophysical Properties of 8a−n in THF

compd	Ar	$\lambda_{abs}{}^a$ (nm)	log ε	$\lambda_{em}{}^b$ (nm)	$\Delta\lambda_{stokes}{}^c$ (nm)	$\Phi_f{}^d$	τ_f (ns)^e
8a	4-pyridyl	296, 372, 407	4.66, 4.38, 4.38	456	49	0.42	2.24
8b	4-trifluoromethyl-phenyl	299, 373, 404	4.72, 4.43, 4.43	458	54	0.45	2.43
8c	4-cyano-phenyl	304, 375, 409	4.78, 4.50, 4.53	460	51	0.51	2.10
8d	4-nitryl-phenyl	283, 376, 409	4.77, 4.51, 4.54	461	52	0.11	1.43
8e	4-formyl-phenyl	310, 376, 414	4.74, 4.52, 4.57	462	48	0.52	1.83
8f	4-chloro-phenyl	296, 375, 406	4.72, 4.46, 4.46	466	60	0.52	3.05
8g	4-fluoro-phenyl	293, 374, 405	4.72, 4.48, 4.47	468	63	0.52	3.77
8h	phenyl	294, 375, 405	4.67, 4.42, 4.41	469	64	0.53	3.87
8i	4-methyl-phenyl	296, 377, 411	4.70, 4.46, 4.47	476	65	0.67	3.92
8j	3-thienyl	299, 383, 417	4.63, 4.40, 4.42	487	70	0.55	3.42
8k	4-methoxy-phenyl	296, 382, 417	4.71, 4.50, 4.51	493	76	0.59	4.42
8l	2-thienyl	315, 398, 433	4.69, 4.51, 4.57	505	72	0.53	3.18
8m	triphenylamine	310, 428	4.89, 4.59	563	135	0.12	4.14
8n	4-N,N-dimethyl-phenyl	309, 440	4.72, 4.51	593	153	0.02	1.01

^{a}The maximum absorption bands (1 × 10^{-5} M) were only shown. ^{b}Excited at the longest maximum absorption peak. ^{c}Stokes shift = $\lambda_{max}{}^{em} - \lambda_{max}{}^{abs}$. ^{d}Perylene as the standard (cyclohexane, 0.98).[36,37] ^{e}Fluorescent lifetime.

electron donating ability of the substituents, the dyes showed not only more red-shift absorption, but also considerably enhanced molar absorption coefficient. Similar to the absorption spectra, the fluorescence spectra of dyes 8a−n also exhibited red-shift emission bands compared with imide 5, and the greater red-shift was found with the increase of the electron-donating ability of the substituents (Figure 4a). Furthermore, it was found that
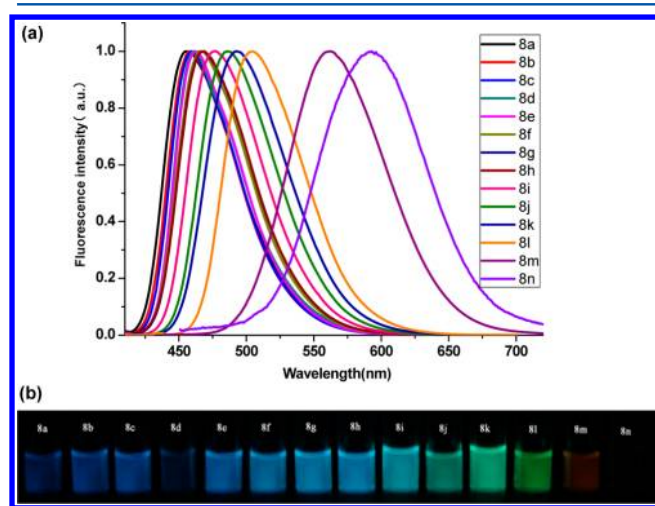

Figure 4. (a) Fluorescence spectra of 8a−n in THF (1 × 10^{-5} M), and (b) the fluorescent image of corresponding solutions under ultraviolet light (365 nm).

these imide dyes had good photoluminescence capabilities with Φ_f values between 0.42 and 0.67 except for 8d (0.12), 8m (0.12), 8n (0.02). The fluorescence images of 8a−n under ultraviolet light (365 nm) showed that most of the colors of the imide dyes were blue, while green, orange and red color for 8l, 8m, and 8n, respectively, could be obviously observed (Figure 4b).

Electrochemical Properties. The electrochemical properties of 8a−n were measured by cyclic voltammetry (CV) in a 0.1 M n-Bu$_4$NPF$_6$ solution in acetonitrile at a scan rate of 100 mV/s at room temperature under the protection of argon, and the corresponding data were summarized in Table 3. Figure 5 shows the cyclic voltammetry curves of 8a−e (left) and 8j−n (right). It was found that all of compounds 8a−n exhibited completely irreversible peaks in both oxidation and reduction

process, which suggested that the ionic species were either very stable or transformed into the electroinactive species. It was also found that the electronic-withdrawing aromatic substituents of 8a−e had main influence on the negative potential region, and made the reduction potential shift to a more positive direction for the electronic-withdrawing groups, which could strengthen the electron affinity ability. Meanwhile, the electronic-donating aromatic substituents of 8j−n had main influence on the positive potential region and made the oxidation potential to a negative direction for the electronic-donating groups, which could reduce the ionization potential. We further found that along with the enhancement of aromatic substituents electron-withdrawing ability, the reduction potential moved more positive, but the oxidation potential moved just the opposite.

Theoretical Studies. In order to get insight into the electronic effects of peripheral aromatic substituents on the imide dyes, we further performed density functional theory (DFT) calculations on compounds 8c, 8h, 8k, and 8l at the B3LYP[39,40]/6-31G(d) level with Gaussian 09 program. It was noted that 8c, 8h, 8k, and 8l successively involve the aromatic substituent of an electron-withdrawing 4-cyano-phenyl, a phenyl, an electron-donating 4-methoxy-phenyl, and a 2-thienyl. The calculated energies including the electron-state-density distribution of the highest occupied molecular orbital (HOMO) and the lowest unoccupied molecular orbital (LUMO) of 8c, 8h, 8k, and 8l were shown in Figure 6 and Figure 7, respectively, and served as the representative systems to study the electronic influences of the aromatic substituents on imide dyes.

Figure 6 showed the optimized geometries with the electron-state density distributions of the LUMO, HOMO, and HOMO-1 for compounds 8c, 8h, 8k, and 8l. We could find that (1) aromatic substituents showed well conjugated effect with the dihydroindeno[2,1-c]fluorene core, which extended the conjugation system greatly; (2) the HOMO-1 orbitals of all compounds were more or less delocalized over the conjugated part of the entire molecule; (3) the electron density of the HOMO were mainly distributed on the peripheral aromatic substituent and also spread over the entire dihydroindeno[2,1-c]fluorene core, while the electron density of the LUMO showed a decrease generally in the electron density on the aromatic substituents moieties and a concomitant increase in

Table 3. Electrochemistry Properties of 8a–n

compd	Ar	E_{ox}^{onset} [a]	E_{red}^{onset} [a]	HOMO[b]	LUMO[b]	E_g [c]
8a	4-pyridyl	1.45	−1.49	−6.26	−3.18	3.08
8b	4-trifluoromethyl-phenyl	1.40	−1.78	−6.21	−2.89	3.32
8c	4-cyano-phenyl	1.27	−1.65	−6.08	−3.02	3.06
8d	4-nitryl-phenyl	1.38	−1.48	−6.19	−3.19	3.00
8e	4-formyl-phenyl	1.13	−1.70	−5.94	−2.97	2.97
8f	4-chloro-phenyl	1.21	−1.72	−6.02	−2.95	3.07
8g	4-fluoro-phenyl	1.25	−2.17	−6.06	−2.50	3.56
8h	phenyl	1.13	−1.75	−5.94	−2.92	3.02
8i	4-methyl-phenyl	1.08	−1.77	−5.89	−2.90	2.99
8j	3-thienyl	0.96	−1.81	−5.77	−2.86	2.91
8k	4-methoxy-phenyl	0.96	−2.04	−5.77	−2.63	3.14
8l	2-thienyl	0.98	−1.99	−5.79	−2.68	3.11
8m	triphenylamine	0.63	−2.07	−5.44	−2.60	2.84
8n	4-N,N-dimethyl-phenyl	0.37	−1.84	−5.18	−2.83	2.35

[a] All potentials are versus Ag/AgNO$_3$. [b] HOMO = $-E^{ox}_{vsFc/Fc+}$ −4.8 eV. LUMO = $-E^{red}_{vsFc/Fc+}$ −4.8 eV. [c] Electrochemical band gaps were determined by $E_g = E_{HOMO} - E_{LUMO}$.
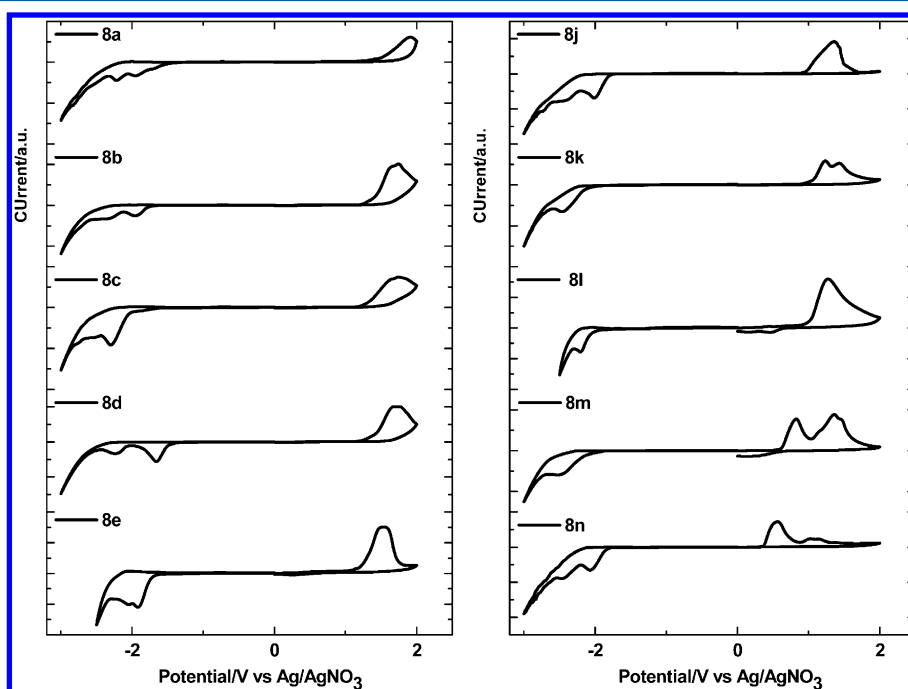

Figure 5. Cyclic voltammograms of **8a–8e** (left) and **8j–n** (right) in n-Bu$_4$NPF$_6$ solution in acetonitrile at a sweep rate of 100 mV/s. Working electrode: Platinum inlaid disk (diameter ∼2 mm). Counter electrode: platinum wire. Reference electrode: Ag/AgNO$_3$ (0.01 M in acetonitrile).

the electron-withdrawing imide moiety; (4) dihydroindeno[2,1-c]fluorene core involving both the HOMO and LUMO orbitals possesses more electron density, which indicates that the dihydroindenofluorene moiety played an important role in the charge transfer process of π−π* conversion from the HOMO to the LUMO orbitals.

Figure 7 shows the calculated energy levels of **8c**, **8h**, **8k**, and **8l**. It was found that aromatic substituent group with electron-withdrawing property (e.g., **8c**) could make the HOMO and LUMO downshift at the same time, but the HOMO downshifts more seriously, which thus made the energy gap of **8c** (3.26 eV) be bigger than that of **8h** (3.20 eV) with electron-donating property. This lower LUMO energy level could explain why the dye with electron-withdrawing aromatic substituent groups showed a more positive reduction potential. Moreover, although the LUMO energy levels in dyes **8l** and **8m** with electron-donating aromatic substituent groups were almost the same as that

of **8h** (less than 0.1 eV), the HOMO energy levels showed an obvious upshift (more than 0.2 eV), which resulted in smaller energy gaps of **8l** (3.05 eV) and **8m** (2.91 eV) than that of **8h** (3.20 eV). These results could also give an explanation in theory to that the aromatic substituent group with electronic-donating property had main influence on the oxidation process of the dye.

■ CONCLUSIONS

In summary, we have developed a new kind of dihydroindeno-[2,1-c]fluorene-based imide dyes. Consequently, a series of the imide dyes were conveniently and efficiently synthesized starting from the commercially available 6-methoxy-2,3-dihydro-1H-inden-1-one. The crystal structure of **8j** showed that the dihydroindeno[2,1-c]fluorene core has an approximate plane structure, and the molecule can pack into a herringbone-like assembly by the head to tail arrangements in the solid state. It was
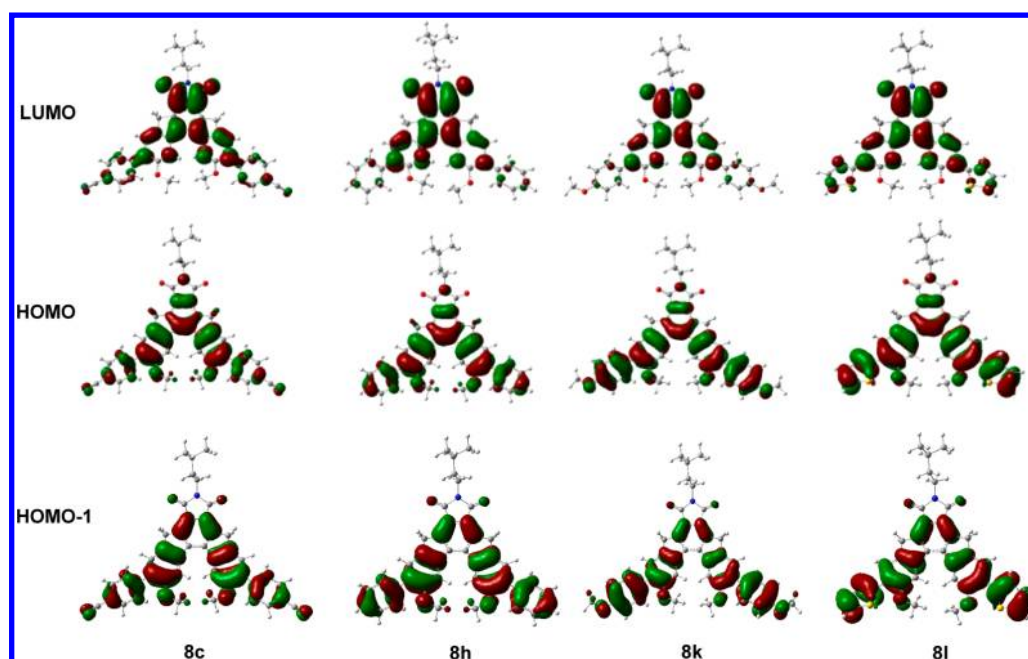
Figure 6. Molecular orbital surfaces of the HOMO-1, HOMO, and LUMO of **8c**, **8h**, **8k**, **8l** obtained at the B3LYP/6-31G(d) level.
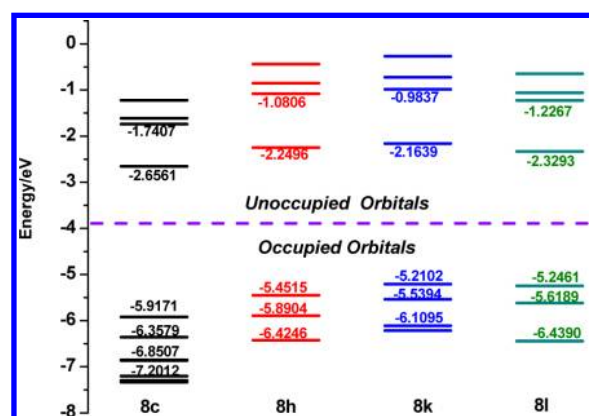

Figure 7. Calculated energy levels of molecular orbitals of **8c**, **8h**, **8k**, and **8l**.

found that these aryl substituted imide dyes showed fluorescent emission from blue to red (456 to 593 nm), and most of them also exhibited moderate to high quantum yields (0.42−0.67), which could thus make them be suitable candidates for organic luminescent materials. Moreover, the electrochemical properties of the aryl-substituted imide dyes were measured by cyclic voltammetry, and they showed great dependent on their structural features. The theoretical calculations were also performed and gave a further explanation for their electrochemical behaviors.

■ EXPERIMENTAL SECTION

6,6′-Dimethoxy-3H,3′H-1,1′-biindene (2). A mixture of activated aluminum flake (3.2 g, 119 mmol), 6-methoxy-2,3-dihydro-1H-inden-1-one **1** (20 g, 123 mmol), toluene (70 mL), absolute ethanol (40 mL), HgCl$_2$ (0.25 g, 0.92 mmol) was heated to reflux for 10 h. After the reaction mixture was cooled to room temperature, aqueous HCl (10%, 100 mL) and excess sulfur were added and vigorously stirred for another 12 h. The mixture was filtrated, and the filtrate was extracted with ethyl acetate (3 × 150 mL). The combined organic layer was washed with water, dried over MgSO$_4$, and then concentrated under reduced pressure to give a residue. To the residue was added anhydride (24 mL) and acetic acid (16 mL), and the

mixture was heated to reflux for 6 h. The remained anhydride and acetic acid were then removed under reduced pressure to give deep red sticky residue, which was dissolved in CH$_2$Cl$_2$ and washed by NaHCO$_3$ aqueous solution (3 × 150 mL). The combined organic layer was washed with water, dried over MgSO$_4$, and then concentrated under reduced pressure to give a residue, which was separated by chromatography with CH$_2$Cl$_2$ and petroleum ether (1:5, v/v) as eluent to give pure diene **2** (7.8 g, 44%) as yellow powder: mp 84−86 °C; ^{1}H NMR (300 MHz, CDCl$_3$) δ 7.37 (d, J = 8.2 Hz, 2H), 7.11 (d, J = 2.4 Hz, 2H), 6.81 (d, J = 2.4 Hz, 1H), 6.78 (d, J = 2.4 Hz, 1H), 6.74 (s, 2H), 3.76 (s, 6H), 3.47 (d, J = 1.5 Hz, 4H); ^{13}C NMR (75 MHz, CDCl$_3$) δ 159.2, 145.9, 139.1, 136.6, 132.9, 124.6, 111.2, 106.8, 55.6, 37.9; HR ESI-MS m/z calcd for [M + H$^+$]$^+$ C$_{20}$H$_{19}$O$_2$, 291.1380, found 291.1380.

2,12-Dimethoxy-5,5a,8b,9-tetrahydroindeno[2′,1′:3,4]-fluoreno[1,2-c]furan-6,8(5bH,8aH)-dione (3). The mixture of diene **2** (4 g, 13.8 mmol) and maleic anhydride (13 g, 138 mmol) was heated at 150 °C for 4 h. The reaction mixture was treated with hot water (50 mL), cooled to room temperature, and then performed by filtration. The crude product was purified by recrystallization with acetic anhydride to give the anhydride **3** (4.2 g, 81%) as pale yellow powder: mp >300 °C; ^{1}H NMR (300 MHz, CDCl$_3$) δ 7.64 (d, J = 2.2 Hz, 2H), 7.23 (d, J = 4.5 Hz, 2H), 6.86 (dd, J = 8.4, 2.3 Hz, 2H), 3.85 (d, J = 3.4 Hz, 8H), 3.59−3.57 (m, 2H), 3.34−3.23 (m, 4H); ^{13}C NMR (125 MHz, CDCl$_3$) δ 171.1, 158.8, 139.7, 139.0, 137.0, 126.2, 115.7, 108.4, 55.6, 43.3, 42.7, 31.3; HR ESI-MS m/z calcd for [M + H$^+$]$^+$ C$_{24}$H$_{21}$O$_5$, 389.1384, found 389.1382.

2,12-Dimethoxyindeno[2′,1′:3,4]fluoreno[1,2-c]furan-6,8-(5H,9H)-dione (4). The mixture of **3** (2 g, 5.15 mmol) and lead tetraacetate (2.2 equiv) in acetic acid and acetic anhydride (1:1, v/v) was stirred at 100 °C for 4 h. After the mixture was cooled to room temperature, water was added and then collected by filtration to give compound **4** (1.8 g, 91%) as yellow powder. Further purification was not performed for its poor solubility: mp >300 °C; HR ESI-MS m/z calcd for [M + H$^+$]$^+$ C$_{24}$H$_{17}$O$_5$, 385.1071, found 385.1072.

7-Isopentyl-2,12-dimethoxy-5H-diindeno[2,1-e:1′,2′-g]-isoindole-6,8(7H,9H)-dione (5). To a solution of compound **4** (200 mg, 0.52 mmol) in DMF under argon was added isoamylamine (10 equiv), and the mixture was stirred at 80 °C for 12 h. The solvent was removed under reduced pressure to give a residue, which was purified by chromatography with CH$_2$Cl$_2$ and petroleum ether (1:1, v/v) as eluent to give compound **5** (212 mg, 90%) as yellowish-green powder: mp 236−237 °C; ^{1}H NMR (300 MHz, CDCl$_3$) δ 7.74 (d, J = 2.0 Hz, 2H), 7.38 (d, J = 8.3 Hz, 2H), 6.89 (dd, J = 8.3, 2.1 Hz, 2H), 3.85

(s, 10H), 3.60 (t, J = 7.5 Hz, 2H), 1.73−1.50 (m, 3H), 0.99 (d, J = 6.4 Hz, 6H); ^{13}C NMR (75 MHz, CDCl$_3$) δ 168.6, 158.8, 142.1, 141.7, 140.7, 137.3, 125.7, 124.1, 114.2, 109.7, 55.6, 37.5, 36.2, 34.6, 26.0, 22.4; HR ESI-MS m/z calcd for [M + H$^+$]$^+$ C$_{29}$H$_{28}$NO$_4$, 454.2013, found 454.2015.

3,11-Dibromo-2,12-dimethoxyindeno[2′,1′:3,4]fluoreno[1,2-c]furan-6,8(5H,9H)-dione (6). To the solution of anhydride **3** (1 g, 2.6 mmol) in CH$_2$Cl$_2$ (100 mL) was added bromine (1 mL) in CH$_2$Cl$_2$ (10 mL) dropwise. After 4 h, sodium hydrogen sulfite was added to the mixture until the color of the mixture was changed into yellow. The solid was collected by filtration to give the dibromo-substituted anhydride **6** (1.2 g, 86%) as a yellow powder: mp >300 °C; ^{1}H NMR (300 MHz, CDCl$_3$) δ 8.05 (s, 2H), 7.94 (s, 2H), 4.30 (s, 4H), 4.06 (s, 6H); ^{13}C NMR (125 MHz, DMSO-d_6) δ 163.4, 155.3, 144.1, 143.1, 139.7, 139.3, 130.5, 124.4, 113.4, 108.5, 57.1, 35.1; HR EI-MS m/z calcd for [M]$^+$ C$_{24}$H$_{14}$Br$_2$O$_5$, 539.9208, found 539.9202.

3,11-Dibromo-7-isopentyl-2,12-dimethoxy-5H-diindeno-[2,1-e:1′,2′-g]isoindole-6,8(7H,9H)-dione (7). The mixture of compound **4** (200 mg, 0.37 mmol), isoamylamine (322 mg, 3.7 mmol), imidazole (6 g) and the quantity of a microspatulum of zinc acetate dehydrate was stirred at 130 °C for 4 h, and then ethanol (100 mL) was added. The reaction mixture was extracted with aqueous CH$_2$Cl$_2$, and the organic layer was concentrated in vacuo to give a residue, which was then purified by chromatography with CH$_2$Cl$_2$ and petroleum ether (1:1, v/v) as eluent to give **7** (192 mg, 85%) as a yellowish-green powder: mp >300 °C; ^{1}H NMR (300 MHz, CDCl$_3$) δ 8.00 (s, 2H), 7.86 (s, 2H), 4.22 (s, 4H), 4.05 (s, 6H), 3.71 (t, J = 7.5 Hz, 2H), 1.61 (m, 3H), 0.99 (d, J = 6.2 Hz, 6H); ^{13}C NMR (125 MHz, CDCl$_3$) δ 168.6, 155.3, 141.7, 140.4, 139.3, 130.3, 125.0, 113.4, 107.8, 57.0, 37.5, 36.5, 34.9, 26.0, 22.4; HR ESI-MS m/z calcd for [M + H$^+$]$^+$ C$_{29}$H$_{26}$Br$_2$NO$_4$, 612.0208, found 612.0195.

General Procedure for Suzuki−Miyaura Cross Coupling. After a mixture of compound **7** (61 mg, 0.1 mmol), K$_2$CO$_3$ (138 mg, 1 mmol), boronic acid (0.3 mmol) in toluene (18 mL), ethanol (12 mL) and water (6 mL) was degassed three times and kept under argon atmosphere, catalytic amount (∼10%) of Pd(PPh$_3$)$_4$ was then added. The resulting mixture was heated to reflux for 8 h, cooled to room temperature, and then poured into 5% aqueous hydrochloric acid (15 mL). The mixture was extracted with dichloromethane (3 × 5 mL), and the combined organic layer was washed with water and dried over anhydrous MgSO$_4$. The solvent was removed in vacuo to give a residue, which was purified by chromatography.

7-Isopentyl-2,12-dimethoxy-3,11-di(pyridin-4-yl)-5H-diindeno[2,1-e:1′,2′-g]isoindole-6,8(7H,9H)-dione (8a). Yellow powder. Yield: 80%; mp 270 °C (dec.); ^{1}H NMR (300 MHz, CDCl$_3$) δ 8.69 (d, J = 5.8 Hz, 4H), 8.09 (s, 2H), 7.62 (s, 2H), 7.55 (d, J = 6.0 Hz, 4H), 4.18 (s, 4H), 3.99 (s, 6H), 3.61 (t, J = 7.5 Hz, 2H), 1.71−1.52 (m, 3H), 0.97 (d, J = 6.3 Hz, 6H); ^{13}C NMR (75 MHz, CDCl$_3$) δ 168.5, 156.2, 149.8, 145.7, 142.1, 142.0, 141.5, 138.5, 128.8, 127.2, 124.7, 124.1, 107.5, 56.4, 37.5, 36.3, 35.0, 26.0, 22.4; HR ESI-MS m/z calcd for [M + H$^+$]$^+$ C$_{39}$H$_{34}$N$_3$O$_4$, 608.2544, found 608.2536.

7-Isopentyl-2,12-dimethoxy-3,11-bis(4-(trifluoromethyl)-phenyl)-5H-diindeno[2,1-e:1′,2′-g]isoindole-6,8(7H,9H)-dione (8b). Pale yellow powder. Yield: 91%; mp 274−275 °C; ^{1}H NMR (300 MHz, CDCl$_3$) δ 8.18 (s, 2H), 7.78−7.67 (m, 8H), 7.64 (s, 2H), 4.28 (s, 4H), 3.98 (s, 6H), 3.70 (t, J = 7.5 Hz, 2H), 1.71−1.57 (m, 3H), 0.99 (d, J = 6.2 Hz, 6H); ^{13}C NMR (75 MHz, CDCl$_3$) δ 168.7, 156.1, 142.2, 141.1, 138.5, 130.4, 129.9, 127.5, 125.11, 125.06, 124.7, 107.5, 56.4, 37.5, 36.4, 35.1, 26.0, 22.4; HR ESI-MS m/z calcd for [M + H$^+$]$^+$ C$_{43}$H$_{34}$F$_6$NO$_4$, 742.2392, found 742.2387.

4,4′-(7-Isopentyl-2,12-dimethoxy-6,8-dioxo-6,7,8,9-tetrahydro-5H-diindeno[2,1-e:1′,2′-g]isoindole-3,11-diyl)-dibenzonitrile (8c). Yellowish-green powder. Yield: 66%; mp 292−294 °C; ^{1}H NMR (300 MHz, CDCl$_3$) δ 8.20 (s, 2H), 7.75 (s, 8H), 7.67 (s, 2H), 4.36 (s, 4H), 3.99 (s, 6H), 3.76 (t, J = 6.0 Hz, 2H), 1.66−1.61 (m, 3H), 1.01 (d, J = 6.2 Hz, 6H); ^{13}C NMR (75 MHz, CDCl$_3$) δ 168.7, 156.1, 142.8, 142.2, 142.1, 141.5, 138.6, 131.9, 130.2, 129.8, 127.4, 124.9, 118.9, 111.0, 107.5, 56.4, 37.5, 36.4, 35.1, 26.0, 22.4; HR ESI-MS m/z calcd for [M + H$^+$]$^+$ C$_{43}$H$_{34}$N$_3$O$_4$, 656.2544, found 656.2541.

7-Isopentyl-2,12-dimethoxy-3,11-bis(4-nitrophenyl)-5H-diindeno[2,1-e:1′,2′-g]isoindole-6,8(7H,9H)-dione (8d). Yellow powder. Yield: 88%; mp 249 °C; ^{1}H NMR (300 MHz, CDCl$_3$) δ 8.32

(d, J = 8.8 Hz, 4H), 8.21 (s, 2H), 7.80 (d, J = 8.8 Hz, 4H), 7.69 (s, 2H), 4.34 (s, 4H), 4.01 (s, 6H), 3.78−3.70 (t, J = 6.0 Hz, 2H), 1.71−1.58 (m, 3H), 1.00 (d, J = 6.2 Hz, 6H); ^{13}C NMR (75 MHz, CDCl$_3$) δ 168.7, 156.1, 147.0, 144.9, 142.23, 142.16, 141.7, 138.6, 130.4, 129.5, 127.5, 125.0, 123.4, 107.4, 56.4, 37.5, 36.5, 35.2, 26.0, 22.4; HR ESI-MS m/z calcd for [M + H$^+$]$^+$ C$_{41}$H$_{34}$N$_3$O$_8$, 696.2340, found 696.2342.

4,4′-(7-Isopentyl-2,12-dimethoxy-6,8-dioxo-6,7,8,9-tetrahydro-5H-diindeno[2,1-e:1′,2′-g]isoindole-3,11-diyl)-dibenzaldehyde (8e). Yellowish-green powder. Yield: 62%; mp 248−250 °C; ^{1}H NMR (300 MHz, CDCl$_3$) δ 10.09 (s, 2H), 8.13 (s, 2H), 7.97 (d, J = 8.2 Hz, 4H), 7.79 (d, J = 8.2 Hz, 4H), 7.63 (s, 2H), 4.21 (s, 4H), 3.99 (s, 6H), 3.63 (t, J = 7.5 Hz, 2H), 1.68−1.58 (m, 3H), 0.97 (d, J = 6.2 Hz, 6H); ^{13}C NMR (75 MHz, CDCl$_3$) δ 191.9, 168.6, 156.2, 144.4, 142.1, 142.0, 141.2, 138.5, 135.2, 130.4, 130.2, 129.6, 127.5, 124.6, 107.6, 56.5, 37.5, 36.4, 35.1, 26.0, 22.4; HR ESI-MS m/z calcd for [M + H$^+$]$^+$ C$_{43}$H$_{36}$NO$_6$, 662.2537, found 662.2537.

3,11-Bis(4-chlorophenyl)-7-isopentyl-2,12-dimethoxy-5H-diindeno[2,1-e:1′,2′-g]isoindole-6,8(7H,9H)-dione (8f). Yellow-ish-green powder. Yield: 93%; mp 296−297 °C; ^{1}H NMR (300 MHz, CDCl$_3$) δ 8.19 (s, 2H), 7.64 (s, 2H), 7.57 (d, J = 8.5 Hz, 4H), 7.44 (d, J = 8.5 Hz, 4H), 4.32 (s, 4H), 3.97 (s, 6H), 3.74 (t, J = 7.5 Hz, 2H), 1.67−1.59 (m, 3H), 1.00 (d, J = 6.2 Hz, 6H); ^{13}C NMR (75 MHz, CDCl$_3$) δ 168.4, 155.9, 141.82, 141.77, 140.3, 138.4, 136.3, 133.5, 130.8, 130.4, 128.4, 127.2, 124.1, 107.5, 56.4, 37.4, 36.2, 34.9, 26.0, 22.3; HR ESI-MS m/z calcd for [M + H$^+$]$^+$ C$_{41}$H$_{34}$Cl$_2$NO$_4$, 674.1859, found 674.1858.

3,11-Bis(4-fluorophenyl)-7-isopentyl-2,12-dimethoxy-5H-diindeno[2,1-e:1′,2′-g]isoindole-6,8(7H,9H)-dione (8g). Yellow-ish-green powder. Yield: 92%; mp 270 °C; ^{1}H NMR (300 MHz, CDCl$_3$) δ 7.98 (s, 2H), 7.56 (t, J = 6.0 Hz, 4H), 7.49 (s, 2H), 7.13 (t, J = 8.5 Hz, 4H), 4.03 (s, 4H), 3.93 (s, 6H), 3.52 (t, J = 7.2 Hz, 2H), 1.66−1.44 (m, 4H), 0.94 (d, J = 6.2 Hz, 6H); ^{13}C NMR (75 MHz, CDCl$_3$) δ 168.6, 164.0, 160.7, 155.9, 141.9, 140.2, 138.4, 133.9, 131.2, 131.1, 130.7, 127.3, 124.2, 115.3, 115.0, 107.5, 56.4, 37.5, 36.2, 34.9, 26.0, 22.4; HR ESI-MS m/z calcd for [M + H$^+$]$^+$ C$_{41}$H$_{34}$F$_2$NO$_4$, 642.2450, found 642.2437.

7-Isopentyl-2,12-dimethoxy-3,11-diphenyl-5H-diindeno-[2,1-e:1′,2′-g]isoindole-6,8(7H,9H)-dione (8h). Yellowish-green powder. Yield: 85%; mp 259−261 °C; ^{1}H NMR (300 MHz, CDCl$_3$) δ 8.13 (s, 2H), 7.63 (s, 2H), 7.61 (s, 4H), 7.46 (t, J = 7.3 Hz, 4H), 7.38 (m, 2H), 4.19 (s, 4H), 3.95 (s, 6H), 3.64 (t, J = 7.5 Hz, 2H), 1.69−1.58 (m, 3H), 0.97 (d, J = 6.3 Hz, 6H); ^{13}C NMR (75 MHz, CDCl$_3$) δ 168.8, 156.1, 142.2, 142.1, 140.3, 138.4, 138.1, 131.9, 129.5, 128.2, 127.6, 127.4, 124.3, 107.6, 56.5, 37.5, 36.3, 35.1, 26.0, 22.4; HR ESI-MS m/z calcd for [M + H$^+$]$^+$ C$_{41}$H$_{36}$NO$_4$, 606.2639, found 606.2637.

7-Isopentyl-2,12-dimethoxy-3,11-di-p-tolyl-5H-diindeno-[2,1-e:1′,2′-g]isoindole-6,8(7H,9H)-dione (8i). Yellowish-green powder. Yield: 85%; mp 250 °C; ^{1}H NMR (300 MHz, CDCl$_3$) δ 8.20 (s, 2H), 7.65 (s, 2H), 7.53 (d, J = 8.1 Hz, 4H), 7.28 (d, J = 8.1 Hz, 4H), 4.31 (s, 4H), 3.96 (s, 6H), 3.74 (t, J = 7.5 Hz, 2H), 2.43 (s, 6H), 1.71−1.59 (m, 3H), 1.00 (d, J = 6.2 Hz, 6H); ^{13}C NMR (75 MHz, CDCl$_3$) δ 168.6, 156.0, 142.0, 141.9, 139.9, 138.3, 137.1, 135.2, 131.7, 129.4, 128.9, 127.4, 124.0, 107.5, 56.4, 37.5, 36.2, 35.0, 26.0, 22.4, 21.3; HR ESI-MS m/z calcd for [M + H$^+$]$^+$ C$_{43}$H$_{40}$NO$_4$, 634.2952, found 634.2945.

7-Isopentyl-2,12-dimethoxy-3,11-di(thiophen-3-yl)-5H-diindeno[2,1-e:1′,2′-g]isoindole-6,8(7H,9H)-dione (8j). Yellow powder. Yield: 95%; mp 296−297 °C; ^{1}H NMR (300 MHz, CDCl$_3$) δ 8.18 (s, 2H), 7.82 (s, 2H), 7.75 (dd, J = 3.0, 1.2 Hz, 2H), 7.55 (dd, J = 5.1, 1.2 Hz, 2H), 7.42 (dd, J = 5.0, 3.0 Hz, 2H), 4.31 (s, 4H), 4.05 (s, 6H), 3.73 (t, J = 7.5 Hz, 2H), 1.69−1.60 (m, 3H), 1.00 (d, J = 6.2 Hz, 6H); ^{13}C NMR (75 MHz, CDCl$_3$) δ 168.2, 155.7, 141.6, 141.4, 139.3, 138.1, 137.7, 128.3, 125.8, 125.6, 124.7, 124.0, 123.6, 107.4, 56.1, 37.4, 36.1, 34.7, 26.1, 22.3; HR ESI-MS m/z calcd for [M + H$^+$]$^+$ C$_{37}$H$_{32}$NO$_4$S$_2$, 618.1767, found 618.1766.

7-Isopentyl-2,12-dimethoxy-3,11-bis(4-methoxyphenyl)-5H-diindeno[2,1-e:1′,2′-g]isoindole-6,8(7H,9H)-dione (8k). Yellow powder. Yield: 74%; mp 233 °C; ^{1}H NMR (300 MHz, CDCl$_3$) δ 7.98 (s, 2H), 7.54 (d, J = 8.6 Hz, 4H), 7.49 (s, 2H), 6.98 (d, J = 8.6 Hz, 4H),

4.01 (s, 4H), 3.92 (s, 6H), 3.88 (s, 6H), 3.51 (t, J = 7.5 Hz, 2H), 1.63 − 1.44 (m, 3H), 0.94 (d, J = 6.4 Hz, 6H); ^{13}C NMR (75 MHz, CDCl$_3$) δ 168.6, 159.1, 156.0, 141.94, 141.90, 139.7, 138.4, 131.3, 130.7, 130.4, 127.2, 124.0, 113.7, 107.6, 56.4, 55.3, 37.5, 36.2, 34.9, 26.0, 22.4; HR ESI-MS m/z calcd for [M + H$^+$]$^+$ C$_{43}$H$_{40}$NO$_6$, 666.2850, found 666.2850.

7-Isopentyl-2,12-dimethoxy-3,11-di(thiophen-2-yl)-5*H*-diindeno[2,1-*e*:1′,2′-*g*]isoindole-6,8(7*H*,9*H*)-dionen (8l). Yellow powder. Yield: 83%; mp 271−272 °C; ^{1}H NMR (300 MHz, CDCl$_3$) δ 8.10 (s, 2H), 7.92 (s, 2H), 7.63 (dd, J = 3.7, 1.1 Hz, 2H), 7.41 (dd, J = 5.1, 1.0 Hz, 2H), 7.15 (dd, J = 5.1, 3.7 Hz, 2H), 4.22 (s, 4H), 4.10 (s, 6H), 3.67 (t, J = 6.0 Hz, 2H), 1.74−1.56 (m, 3H), 0.98 (d, J = 6.3 Hz, 6H); ^{13}C NMR (75 MHz, CDCl$_3$) δ 168.7, 155.0, 142.0, 141.8, 139.8, 138.9, 138.4, 127.0, 126.4, 126.0, 124.6, 124.3, 124.2, 107.6, 56.3, 37.5, 36.3, 35.0, 26.0, 22.4; HR ESI-MS m/z calcd for [M + H$^+$]$^+$ C$_{37}$H$_{32}$NO$_4$S$_2$, 618.1773, found 618.1767.

3,11-Bis(4-(diphenylamino)phenyl)-7-isopentyl-2,12-dimethoxy-5*H*-diindeno[2,1-*e*:1′,2′-*g*]isoindole-6,8(7*H*,9*H*)-dione (8m). Orange powder. Yield: 65%; mp >300 °C; ^{1}H NMR (300 MHz, CD$_2$Cl$_2$) δ 8.11 (s, 2H), 7.60 (s, 2H), 7.54−6.83 (m, 28H), 4.20 (s, 4H), 3.92 (s, 6H), 3.62 (t, J = 7.1 Hz, 2H), 1.57−1.48 (m, 3H), 0.91 (d, J = 6.3 Hz, 6H); mp 236−237 °C; ^{13}C NMR (75 MHz, CDCl$_3$) δ 168.8, 156.0, 147.7, 147.1, 142.12, 142.06, 139.8, 138.5, 131.8 131.3, 130.3, 129.3, 127.2, 124.7, 124.1, 123.1, 122.9, 107.5, 56.4, 37.5, 36.3, 35.1, 26.0, 22.4; HR ESI-MS m/z calcd for [M + H$^+$]$^+$ C$_{65}$H$_{54}$N$_3$O$_4$, 940.4114, found 940.4107.

3,11-Bis(4-(dimethylamino)phenyl)-7-isopentyl-2,12-dimethoxy-5*H*-diindeno[2,1-*e*:1′,2′-*g*]isoindole-6,8(7*H*,9*H*)-dione (8n). Red powder. Yield: 80%; mp 255 °C; ^{1}H NMR (300 MHz, CDCl$_3$) δ 8.20 (s, 2H), 7.65 (s, 2H), 7.57 (d, J = 8.8 Hz, 4H), 6.83 (d, J = 8.9 Hz, 4H), 4.30 (s, 4H), 3.97 (s, 6H), 3.74 (t, J = 7.1 Hz, 2H), 3.03 (s, 12H), 1.67−1.59 (m, 3H), 1.00 (d, J = 6.2 Hz, 6H); ^{13}C NMR (75 MHz, CDCl$_3$) δ 168.8, 156.0, 149.9, 142.00, 141.96, 139.1, 138.5, 131.9, 130.3, 126.9, 126.0, 123.8, 112.2, 107.7, 56.4, 40.5, 37.5, 36.2, 35.0, 26.0, 22.4; HR ESI-MS m/z calcd for [M + H$^+$]$^+$ C$_{45}$H$_{46}$N$_3$O$_4$, 692.3483, found 692.3473.

Computational Methods. DFT calculations were performed with the Gaussian 09 program package. The geometries were optimized using the B3LYP method with the 6-31G(d) (for C, H, and O). The natures of the stationary points were assessed by means of vibration frequency analysis.

ASSOCIATED CONTENT

Ⓢ Supporting Information

Copies of ^{1}H and ^{13}C NMR spectra for new compounds; the UV−vis absorption spectra of **8h** in different solvents and **8a−n** in THF; the cyclic voltammograms of **8f−i**; the DFT calculation data of **8c**, **8h**, **8k**, **8l**; and the crystallographic information file (CIF) for **8j**. These materials are available free of charge via the Internet at http://pubs.acs.org.

AUTHOR INFORMATION

Corresponding Authors
*E-mail: haiyanlu@ucas.ac.cn
*E-mail: cchen@iccas.ac.cn

Notes
The authors declare no competing financial interest.

ACKNOWLEDGMENTS

REFERENCES

(1) Romain, M.; Tondelier, D.; Vanel, J.-C.; Geffroy, B.; Jeannin, O.; Rault-Berthelot, J.; Métivier, R.; Poriel, C. *Angew. Chem., Int. Ed.* **2013**, *52*, 14147−14151.

(2) Fix, A. G.; Deal, P. E.; Vonnegut, C. L.; Rose, B. D.; Zakharov, L. N.; Haley, M. M. *Org. Lett.* **2013**, *15*, 1362−1365.

(3) Fix, A. G.; Chase, D. T.; Haley, M. M. In *Topics in Current Chemistry*; Siegel, J. S., Wu, Y.-T., Eds.; Springer: Berlin, Germany, in press (DOI: 10.1007/128_2012_376).

(4) Grimsdale, A. C.; Müllen, K. *Macromol. Rapid Commun.* **2007**, *28*, 1676−1702.

(5) Thirion, D.; Poriel, C.; Rault-Berthelot, J.; Barriere, F.; Jeannin, O. *Chem.—Eur. J.* **2010**, *16*, 13646−13658.

(6) Chase, D. T.; Fix, A. G.; Kang, S. J.; Rose, B. D.; Weber, C. D.; Zhong, Y.; Zakharov, L. N.; Lonergan, M. C.; Nuckolls, C.; Haley, M. M. *J. Am. Chem. Soc.* **2012**, *134*, 10349−10352.

(7) Usta, H.; Facchetti, A.; Marks, T. J. *J. Am. Chem. Soc.* **2008**, *130*, 8580−8581.

(8) Merlet, S.; Birau, M.; Wang, Z. Y. *Org. Lett.* **2002**, *4*, 2157−2159.

(9) Hadizad, T.; Zhang, J.; Wang, Z. Y.; Gorjanc, T. C.; Py, C. *Org. Lett.* **2005**, *7*, 795−797.

(10) Ku, S.-Y.; Chi, L.-C.; Hung, W.-Y.; Yang, S.-W.; Tsai, T.-C.; Wong, K.-T.; Chen, Y.-H.; Wu, C.-I. *J. Mater. Chem.* **2009**, *19*, 773−780.

(11) Kim, J.; Kim, S. H.; Jung, I. H.; Jeong, E.; Xia, Y.; Cho, S.; Hwang, I.-W.; Lee, K.; Suh, H.; Shim, H.-K.; Woo, H. Y. *J. Mater. Chem.* **2010**, *20*, 1577−1586.

(12) Park, Y.-I.; Lee, J. S.; Kim, B. J.; Kim, B.; Lee, J.; Kim, D. H.; Oh, S.-Y.; Cho, J. H.; Park, J.-W. *Chem. Mater.* **2011**, *23*, 4038−4044.

(13) Shen, Y.; Chen, C. F. *Chem. Rev.* **2012**, *112*, 1463−1535.

(14) Du, B.; Wang, L.; Yuan, S.-C.; Lei, T.; Pei, J.; Cao, Y. *Polymer* **2013**, *54*, 2935−2944.

(15) Yang, Y.; Petersen, J. L.; Wang, K. K. *J. Org. Chem.* **2003**, *68*, 5832−5837.

(16) Hilt, G.; Paul, A.; Harms, K. *J. Org. Chem.* **2008**, *73*, 5187−5190.

(17) Youngs, W. J.; Djebli, A.; Tessier, C. A. *Organometallics* **1991**, *10*, 2089−2090.

(18) Altman, Y.; Ginsburg, D. *J. Chem. Soc.* **1961**, 1498−1505.

(19) Keerthi, A.; Liu, Y.; Wang, Q.; Valiyaveettil, S. *Chem.—Eur. J.* **2012**, *18*, 11669−11676.

(20) Li, C.; Schoneboom, J.; Liu, Z.; Pschirer, N. G.; Erk, P.; Herrmann, A.; Mullen, K. *Chem.—Eur. J.* **2009**, *15*, 878−884.

(21) Huang, C.; Barlow, S.; Marder, S. R. *J. Org. Chem.* **2011**, *76*, 2386−2407.

(22) Jiang, W.; Li, Y.; Yue, W.; Zhen, Y. G.; Qu, J. Q.; Wang, Z. H. *Org. Lett.* **2009**, *12*, 228−231.

(23) Zhen, Y. G.; Wang, C. R.; Wang, Z. H. *Chem. Commun.* **2010**, *46*, 1926−1928.

(24) Lei Cui, L.; Zhong, Y.; Zhu, W.; Xu, Y.; Du, Q.; Wang, X.; Qian, X.; Xiao, Y. *Org. Lett.* **2011**, *13*, 928−931.

(25) Yan, H.; Chen, Z.; Zheng, Y.; Newman, C.; Quinn, J. R.; Dotz, F.; Kastler, M.; Facchetti, A. *Nature* **2009**, *457*, 679−686.

(26) Polander, L. E.; Barlow, S.; Seifried, B. M.; Marder, S. R. *J. Org. Chem.* **2012**, *77*, 9426−9428.

(27) Polander, L. E.; Tiwari, S. P.; Pandey, L.; Seifried, B. M.; Zhang, Q.; Barlow, S.; Risko, C.; Brédas, J.-L.; Kippelen, B.; Marder, S. R. *Chem. Mater.* **2011**, *23*, 3408−3410.

(28) Tyson, D. S.; Carbaugh, A. D.; Ilhan, F.; Santos-Pérez, J.; Meador, M. A. *Chem. Mater.* **2008**, *20*, 6595−6596.

(29) Mohebbi, A. R.; Munoz, C.; Wudl, F. *Org. Lett.* **2011**, *13*, 2560−2563.

(30) Bullock, J. E.; Vagnini, M. T.; Ramanan, C.; Co, D. T.; Wilson, T. M.; Dicke, J. W.; Marks, T. J.; Wasielewski, M. R. *J. Phys. Chem. B* **2010**, *114*, 1794−1802.

(31) Erten-Ela, S.; Turkmen, G. *Renew. Energy* **2011**, *36*, 1821−1825.

(32) Imahori, H.; Umeyama, T.; Ito, S. *Acc. Chem. Res.* **2009**, *42*, 1809−1818.

(33) Langhals, H.; Christian, S.; Hofer, A. *J. Org. Chem.* **2013**, *78*, 9883−9891.

(34) Zhan, X.; Facchetti, A.; Barlow, S.; Marks, T. J.; Ratner, M. A.; Wasielewski, M. R.; Marder, S. R. *Adv. Mater.* **2011**, *23*, 268−284.

(35) Chang, J.; Qu, H.; Ooi, Z. E.; Zhang, J.; Chen, Z.; Wu, J.; Chi, C. *J. Mater. Chem. C* **2013**, *1*, 456−462.

(36) Chen, J. D.; Lu, H. Y.; Chen, C. F. *Chem.—Eur. J.* **2010**, *16*, 11843−11846.

(37) Crosby, G. A.; Demas, J. N. *J. Phys. Chem.* **1971**, *75*, 991−1024.

(38) Zagranyarski, Y.; Chen, L.; Zhao, Y.; Wonneberger, H.; Li, C.; Mullen, K. *Org. Lett.* **2012**, *14*, 5444−5447.

(39) Lee, C.; Yang, W.; Parr, R. G. *Phys. Rev. B* **1988**, *37*, 785−789.

(40) Becke, A. D. *J. Chem. Phys.* **1993**, *98*, 5648−5652.